First-principles study of the structural and electronic properties of graphene/MoS_2 interfaces

Nguyen Ngoc Hieu,[1] Huynh Vinh Phuc,[2] Victor V. Ilyasov,[3] Nguyen D. Chien,[4] Nikolai A. Poklonski,[5] Nguyen Van Hieu,[6] and Chuong V. Nguyen[1,7,a)]
[1]*Institute of Research and Development, Duy Tan University, Da Nang, Vietnam*
[2]*Division of Theoretical Physics, Dong Thap University, Dong Thap, Vietnam*
[3]*Department of Physics, Don State Technical University, Rostov on Don, Russia*
[4]*School of Engineering Physics, Hanoi University of Science and Technology, Ha Noi, Vietnam*
[5]*Department of Physics, Belarusian State University, Minsk, Belarus*
[6]*Department of Physics, University of Education, The University of Da Nang, Da Nang, Vietnam*
[7]*Department of Materials Science and Engineering, Le Quy Don Technical University, Ha Noi, Vietnam*

(Received 16 May 2017; accepted 25 August 2017; published online 8 September 2017)

In this paper, we study the structural and electronic properties of graphene adsorbed on MoS_2 monolayer (G/MoS_2) with different stacking configurations using dispersion-corrected density functional theory. Our calculations show that the interaction between graphene and MoS_2 monolayer is a weak van der Waals interaction in all four stacking configurations with the binding energy per carbon atom of −30 meV. In the presence of MoS_2 monolayer, the linear bands on the Dirac cone of graphene at the interfaces are slightly split. A band gap about 3 meV opens in G/MoS_2 interfaces due to the breaking of sublattice symmetry by the intrinsic interface dipole, and it could be effectively modulated by the stacking configurations. Furthermore, we found that an *n*-type Schottky contact is formed at the G/MoS_2 interface in all four stacking configurations with a small Schottky barrier about 0.49 eV. The appearance of the non-zero band gap in graphene has opened up new possibilities for its application in electronic devices such as graphene field-effect transistors. *Published by AIP Publishing*. [http://dx.doi.org/10.1063/1.5001558]

I. INTRODUCTION

Graphene is a two-dimensional sp^2-hybridized carbon monolayer which has been considered as a promising materials for future applications in the nanoelectronics and optoelectronic devices[1,2] due to its extraordinary electronic properties and high carrier mobility.[3–5] However, graphene is a gap-less semiconductor being the biggest problems for applications in graphene-based electronic devices. Furthermore, electronic properties of graphene are very sensitive to external conditions in preparation and synthesis conditions, such as the effects of the impurities[6,7] and external electric field[8] or the graphene-substrate interactions.[9–11] There exist many accessible ways to open the band gap of graphene, one of them is mixing or hybridizing the electronic states at K and K' by breaking translational symmetry at Dirac point of π and π^* energy bands. Another way is breaking the sublattice symmetry in graphene. The simplest way is controlling and modulating the band gap of graphene by placing graphene on a substrate. Besides, substrates are also an essential component of proposed graphene based electronic devices. Also, monolayer MoS_2, graphene-like material, is one of the most studied transition metal dichalcogenide family.[12–15] Unlike gap-less graphene, MoS_2 monolayer is a direct band gap semiconductor with a band gap of 1.8 eV.[16] The MoS_2 monolayer has a high on/off current ratio of 10^8 and high carrier mobility of 200 cm^2/Vs at room temperature,[17] which indicates that MoS_2 monolayer has great potential applications in field-effect transistors (FET) and photodetectors.[18,19]

The graphene/substrate (G/substrate) interfaces have been studied by both theoretical and experimental research groups, using G/h-BN,[20–22] G/ZnO,[23,24] G/P[25–27] G/MoS_2 (Refs. 28 and 29) or G/MnO surfaces.[30] These graphene-based van der Waals (vdW) heterostructures show some novel properties for creating individual components in electronic devices.[31] The G/MoS_2 interfaces have successfully been synthesized experimentally, and they become potential candidate for applications in electronic, photovoltaic and memory devices.[32–34] We have recently studied the electronic and magnetic properties of graphene nanoribbon placed on semiconductor substrate systems using density functional theory (DFT).[35–38] However, the detailed computational studies of electronic properties of G/MoS_2 interface in comparison with experimental results is still unclear and should be further studied. Therefore, in this work, we investigate the electronic properties of interaction between graphene and MoS_2 monolayer, i.e., G/MoS_2 interface using first-principles calculations with vdW corrections. The interaction between graphene and MoS_2 monolayer is characterized by weak vdW interaction at the equilibrium state. The changes in band structures of G/MoS_2 interface with different stacking configurations have also been studied. We believe that our results may provide some potential ways for applications in vdW based field effect transistors (FETs).

II. COMPUTATIONAL METHOD DETAILS

To consider the structural and electronic properties of graphene and MoS_2 interface, the density functional theory

a)Electronic mail: chuongnguyen11@gmail.com

(DFT) calculations were carried out by the Quantum Espresso Package.[39] The general gradient approximation (GGA) in the Perdew-Burke-Ernzerhof (PBE)[40] form has been used for the exchange-correlation energy of the interacting electrons with the frozen-core full-potential projector augmented wave (PAW) method. The kinetic cut-off energy of electron wave functions is 410 eV in the calculations. The $(9 \times 9 \times 1)$ k-point meshes are used for Brillouin zone. All structures were relaxed with the atomic forces on each ion of less than 0.01 eV/Å. A vacuum layer of 22 Å is used in the direction normal to the interface, representing the isolated slab boundary condition.

It is well known that the weak interactions are not well described by the standard PBE functional; a semi-empirical dispersion-corrected density functional theory (DFT-D2) approach proposed by Grimme was adopted.[41] As known that the DFT-D2 method has widely used and demonstrated to give a better description of weak van der Waals (vdW) interactions. The long-range dispersion, the vdW interaction was described by a damped interatomic potential.

The interface between graphene and monolayer MoS_2 is calculated by using a supercell as shown in Fig. 1. The supercell contains one graphene layer and one MoS_2 monolayer. The (4×4) MoS_2 monolayer was used to match (5×5) graphene sheet. In this work, we chose a lateral lattice parameters of supercell $a = 12.30$ Å, which was optimized for freestanding graphene. The lattice mismatch for G/MoS_2 interface was only about 2%, which is reasonably small, and thus it does not affect main results. We consider four representative arrangements of graphene on MoS_2: (i) one C atom of graphene located directly on the top of an S atom and one Mo atom centered below the graphene hexagonal ring [GS-M configuration, Fig. 1(a)]; (ii) one C atom of graphene located directly on the top of a Mo atom and one S atom centered below the graphene hexagonal ring [GM-S configuration, Fig. 1(b)]; (iii) one C atom of graphene located directly on the top of a S atom and one of the graphene hexagonal ring centered above the Mo-S hexagonal ring [GS-G configuration, Fig. 1(c)]; and (iv) one C atom of graphene located directly on the top of a Mo atom and one of the graphene hexagonal ring centered above the Mo-S hexagonal ring [GM-G configuration, Fig. 1(d)].

To determine the stability of graphene and MoS_2 monolayer, the binding energy of the interface is calculated as $E_b = [E_{G/MoS_2} - (E_G + E_{MoS_2})/N]$, where E_{G/MoS_2}, E_G, and E_{MoS_2} are total energy of G/MoS_2 interface, freestanding graphene, and MoS_2 monolayer, respectively. $N = 50$ is the number of carbon atoms in the unit cell of the interface. In this work, we also carry out the spin-polarized calculation. Our results indicate that the G/MoS_2 interfaces are nonmagnetic.

III. RESULTS AND DISCUSSION

We study the effect of MoS_2 monolayer on the structural and electronic properties of graphene. All structures of G/MoS_2 interface have been optimized by using DFT–D2 method with the vdW interaction between two layers. It is well known that the lattice constant of freestanding graphene is about 20% smaller than the one of the isolated MoS_2 monolayer. Therefore, we constructed a supercell consisting of a (5×5) layer graphene (50 C atoms) coated with a (4×4) monolayer MoS_2 (16 Mo atoms and 32 S atoms) with four different stacking configurations to take into account for this lattice mismatch. The remaining lattice mismatch is only about 2%, which is small and it does not effect on the electronic structures in the interfaces. Figure 1 shows the fully relaxed atomic structures of the four interface configurations of graphene adsorbed on MoS_2 substrate. Note that in all four interface configurations, graphene keeps its plane and hexagonal atomic ring. The interlayer distances between graphene layer and top S-layer (d_1) and second S-layer (d_2) are obtained as resulting of the optimized structures. They are listed in Table I. We can see that these distances are similar to the relaxed equilibrium distances of other graphene/substrate interface, which are typical in the vdW-based interfaces, such as G/ZnO[23] and G/phosphorene.[25–27] This indicates that the graphene/substrate interaction is a weak interlayer bonding of vdW-type.

To determine the stability of G/MoS_2 interface, we also calculate the binding energy per C atom between graphene and MoS_2 substrate. As shown in Table I, the average binding energy per C atom is about −32.4 meV/atom, which is close to the binding energy per C atom in 2D van-der-Waals (vdW) interfaces, such as graphene/SnS,[42] graphene/h-BN,[43] and graphene/WSe_2,[44] and graphene/MoS_2.[29] This binding energy also indicates that the graphene-MoS_2 interaction is in the range of van der Waals force. The binding energy per C atom for GS-M, GM-S, GS-G, and GM-G is −29.51 meV,

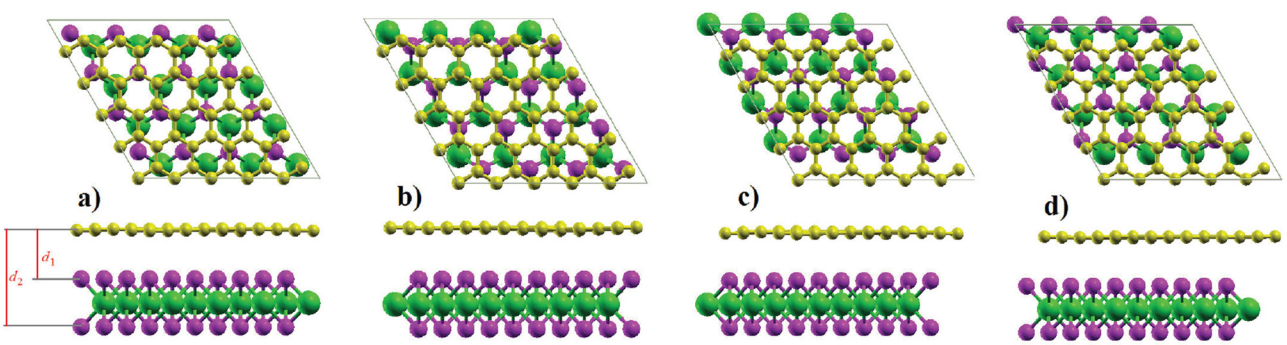

FIG. 1. Top and side views of four different stacking arrangements of graphene adsorbed on MoS_2 monolayer: (a) GS-M configuration, (b) GM-S configuration, (c) GS-G configuration, and (d) GM-G configuration. The green, violet, and yellow balls represent S, Mo, and C atoms, respectively. The distances d_1 and d_2 are, respectively, the interlayer distances between graphene layer and top and bottom S layers in MoS_2 substrate.

TABLE I. The average distances (Å) between graphene layer and top layer d_1 and bottom layer d_2 of MoS_2 monolayer, the binding energy per C atom between graphene and MoS_2 substrate E_b (meV/atom), and the opening band gap E_g (meV) of the G/MoS_2 interface with different stacking configurations.

Configuration	d_1	d_2	E_b	E_g
GS-M	3.34	6.55	−29.51	2.8
GM-S	3.31	6.55	−31.25	3.8
GS-G	3.34	6.52	−30.24	3.6
GM-G	3.36	6.57	−26.11	2.1

−31.25 meV, −30.24 meV, and −26.11 meV, respectively. This binding energy per C atom shows that the GM-G stacking confguration is the most stable configuration. As also mentioned above, the interlayer distance between graphene and the topmost S-layer varies from 3.31 Å to 3.36 Å which depends on stacking configurations. These distances are larger than the sum of the covalent radius of C and S atoms, 1.81 Å. This suggests that the van der Waals interactions between graphene and MoS_2 substrate could be the primary interactions.

To calculate the effect of the stacking configurations on the band gap and electronic properties of G/MoS_2 interface, we calculate the structural and electronic properties of the freestanding graphene sheet and MoS_2 monolayer individually. Our calculations show that the length of graphene primitive cell is 2.46 Å, which is in good agreement with previous reports.[45,46] The isolated graphene has a zero-gap, which is illustrated in Fig. 2(a). Band structure of isolated graphene shows a linear Dirac dispersion around the Fermi level. Figure 2(b) shows the band structure of MoS_2 monolayer. As shown in Fig. 2(b), MoS_2 has a direct band gap of 1.70 eV with the conduction band minimum (CBM) and the valence band maximum (VBM) located at the K point. This band gap is still smaller than that of the experimental study using complementary techniques of optical absorption, photoluminescence, and photoconductivity (1.80 eV).[16] The band gap problem can be addressed more accurately by using a GW approximation. In the present work, however, we do not focus on this problem. This trend is not generalized and more often depends on the material. In this work, we only focus on effects of MoS_2 monolayer substrate on structural and electronic properties of graphene. We believe that the semi-empirical DFT-D2 method is a suitable method for calculations of the G/MoS_2 interface and a new idea of the trends can be obtained from our results.

In Fig. 2(c), we show the partial density of states (PDOS) of C2p_z orbitals in graphene and S3p and Mo4d orbitals in MoS_2 monolayer. It can be see that the bottom of the conduction band is mainly contributed by Mo-d orbitals and the top of the valence band is contributed by Mo-d and S-p orbitals. Mo-d and S-p orbitals are hybridized with each other at the top of the valence band. Figure 2(c) also shows the PDOS of the $2p_z$ state of carbon atom in freestanding graphene. From Fig. 2(c), we can see that the half-filled $2p_z$ orbitals perpendicular to the planar structure form the π and π^* bands in the electronic structure of graphene. The bonding and antibonding bands touch at a single point exactly at the Fermi energy at the hexagonal corner of the graphene's Brillouin zone (K-points).

In Fig. 3, we show the average Coulomb potential for the G/MoS_2 system. We can see that the potential distribution of the substrate does not suffer from the change in the presence of isolated graphene. The high potential barrier has been observed between positions of C atom in isolated graphene surface and S atoms in MoS_2 surface. The difference in work function in the case of G/MoS_2 and isolated MoS_2 surface is defined as $\Delta W = W_{G/MoS_2} - W_{MoS_2}$, and it is about 0.12 eV. As $\Delta W > 0$, electrons will be transferred from graphene to MoS_2 surface, making the n-type contact.

The electronic energy band structures of G/MoS_2 interface of the all four stacking configurations are shown in Fig. 4. Compared with the band structures of freestanding graphene and monolayer MoS_2 (see Fig. 2), the electronic structures of the G/MoS_2 interfaces in all four configurations seem to be a simple sum of each constituent. It is also shown that the linear Dirac-like dispersion relation around the Fermi level of graphene is still preserved in G/MoS_2 interface. But focusing on the linear dispersion, we found that the band gap of G/MoS_2 interface is opened at the Dirac K-point of graphene. It means that at the Dirac K-point, the π and π^* bands repulse each other, forming a small energy band gap. The band gap opening in G/MoS_2 interface can be explained by the lattice symmetry between graphene and MoS_2 monolayer. This effect has been also observed in graphene/h-BN interface.[43] Therefore, the G/MoS_2 interface is a semiconductor with a direct narrow energy gap. This indicates the

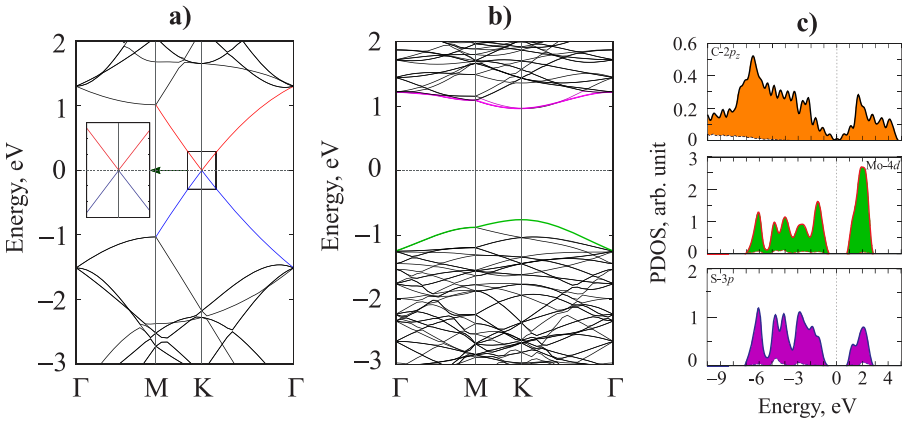

FIG. 2. DFT-D2 calculations of the band structures of: (a) (5 × 5) graphene sheet with the red and blue, respectively, representing the CBM and VBM, (b) (4 × 4) MoS_2 monolayer with the pink and green representing respectively the CBM and VBM, and (c) partial density of states of C-2p_z orbitals in isolated graphene and Mo-4d and S-3p orbitals in MoS_2 monolayer. The Fermi energy level is set to be zero.

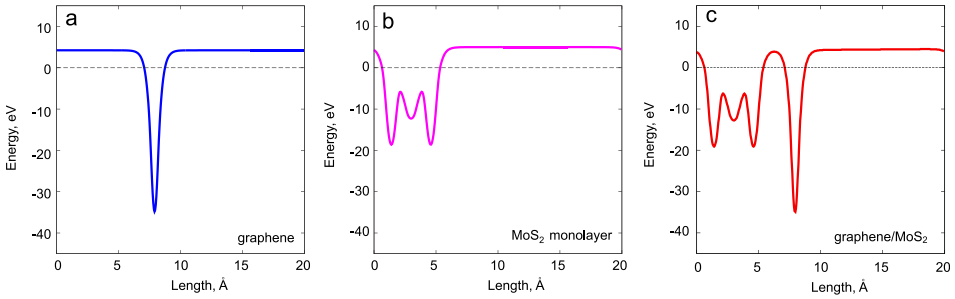

FIG. 3. The plane averaged electrostatic potentials of freestanding graphene (a), isolated monolayer MoS_2 (b), and their G/MoS_2 interface (c) along z-direction.

effect of MoS_2 substrate on the electronic properties of graphene. It suggests that MoS_2 substrate can be used as an ideal substrate for graphene-based device applications. The small band gaps of G/MoS_2 interfaces for GM-S, GS-M, GM-G, and GS-G stacking configurations are 2.8 meV, 3.8 meV, 3.6 meV, and 2.1 meV, respectively, which is in good agreement with the previous result[29] (see the insets in Fig. 4). However, this gap is smaller than that of G/hBN,[22,43] G/sapphire,[47] and G/SiO_2[48] systems.

Also, we found that the GM-S stacking configuration has the largest opened band gap and the lowest binding energy per C atom in comparison with the others. As mentioned above, the nature of this gap is the breaking of sublattice symmetry owing to the graphene-substrate interaction. As shown in Table I, we can see that the GM-S stacking configuration has also the shortest vertical interlayer distance $d_1 = 3.31$ Å. However, the lowest interface distance $d_2 = 6.52$ Å has observed in the GS-G stacking configuration. Additionally, it is well-known that the band gap of graphene-substrate interface strongly depends on the interlayer coupling d_1. With the decreasing interlayer distance d_1, the band gap of graphene will increase. This effect has also been observed in other graphene/substrate interfaces, such as G/h-BN.[49]

In particular, the states forming the top of the valence band of the clean MoS_2 monolayer are shifted upward by an energy about 0.37 eV. While the states of the conduction band minimum are downshifted by an energy about 0.37 eV for all stacking configurations. In many respects, the location of the bands in graphene remains unchanging, in particular, the location and shape of the σ and π bands responsible for the electrical conductivity of the material. Nonetheless, some changes in the states of the graphene under the influence of the substrate are observed near the Fermi level. The dominant influence exerted by the MoS_2 substrate on the band structure of the graphene manifests itself in the appearance of an energy gap from 2 meV to 4 meV between the π and π^* bands of the graphene. Figure 4 shows that at the K point, the π and π^* bands repulse each other, which form a small energy gap. Thus, graphene deposited on the semiconductor MoS_2 substrate is characterized by semiconducting with a direct narrow energy gap. These results also indicate the effect of MoS_2 substrate on band gap and electronic properties of graphene. The insets in Fig. 4 show the linear dispersion around Fermi energy level at Dirac point with the valence band maximum and the conduction band minimum in the band structures of G/MoS_2 interface.

Interestingly, in all these configurations of G/MoS_2 interfaces, we found a Schottky contact, which has been formed between graphene and semiconducting MoS_2 substrate, as shown in Fig. 5. The Schottky barrier height (SBH) is one of the most important properties of metal/semiconductor system such as G/MoS_2 because the current flow crossing the system depends strongly on the magnitude of the Schottky barrier. As the graphene contact with the MoS_2 monolayer, the interface becomes unified electronic systems. Even without any charge transfer between the MoS_2 monolayer and graphene systems, there will be a small band bending. The band bending can be defined as $\Delta W = W_G - W_{MoS_2}$, where W_G and W_{MoS_2} are the work functions of the graphene and MoS_2 monolayer,

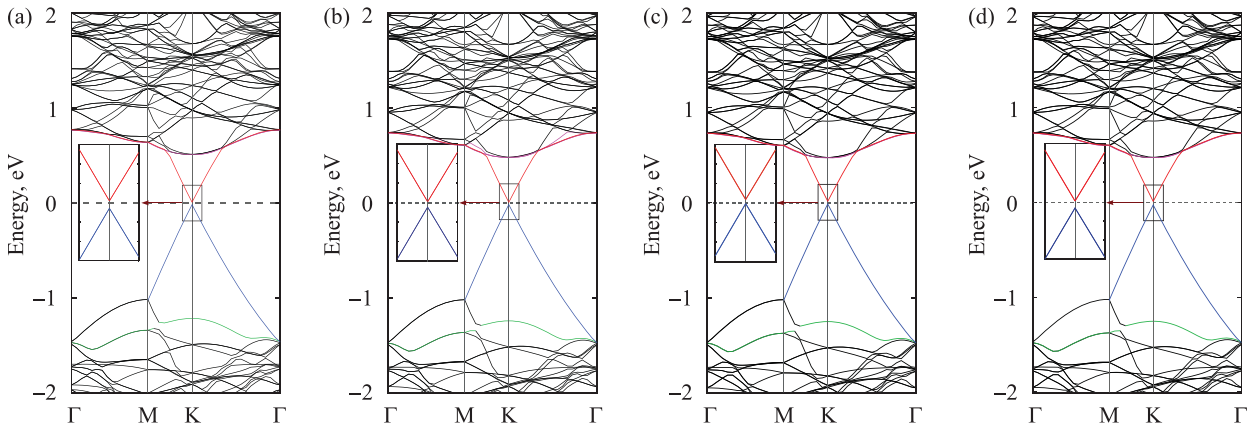

FIG. 4. Band structures of G/MoS_2 interface with different stacking configurations: (a) GS-M configuration, (b) GM-S configuration, (c) GS-G configuration, and (d) GM-G configuration. The Fermi level is set to zero. The energy states around Fermi level from graphene is denoted by red and blue lines for the CBM and VBM, respectively. The insets are the zoom in the bands near Fermi level.

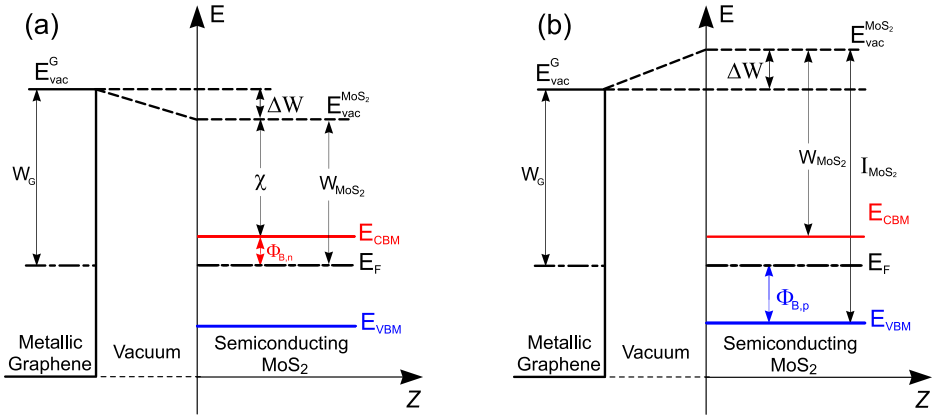

FIG. 5. Schematic energy diagram of (a) *n*-type ($\Delta W > 0$) and (b) *p*-type ($\Delta W < 0$) Schottky barrier height at the G/MoS_2 interface. W_G and W_{MoS_2} are, respectively, the work functions of the graphene and MoS_2 monolayer, E_{CBM} and E_{VBM} are the conduction band minimum and the valence band maximum, respectively, E_F is the Fermi level, $E_{vac}^{G(MoS_2)}$ is the energy of vacuum level of graphene (MoS_2), I_{MoS_2} is the ionization potential of MoS_2, and χ is the electron affinity.

respectively. For the metal/semiconductor interfaces, including G/MoS_2 interface, the semiconducting MoS_2 monolayer have different ionization potentials $I_{MoS_2} = E_{vac}^{MoS_2} - E_{VBM}$ [the energy difference between the vacuum level and the valence band maximum (VBM)] and electron affinity $\chi = E_{vac}^{MoS_2} - E_{CBM}$ [the energy difference between the vacuum level and the conduction band minimum (CBM)], compared to the work function of metallic graphene W_G, forming the Schottky at this type of interfaces. Our calculations shown that the work function of the graphene (W_G) is larger than that of MoS_2 monolayer, that is band bending $\Delta W > 0$, and thus electrons will spontaneously flow from the MoS_2 monolayer to the graphene layer, which demonstrates a *n*-type Schottky barrier contact. The *n*-type Schottky barrier height can be defined as[50] $\Phi_{B,n} = W_G - \chi - \Delta W$, as shown in Fig. 5(a), where χ is the electron affinity of MoS_2 semiconductor. The electron affinity ($\chi = E_{vac} - E_F$) is the energy difference between the vacuum level and the conduction band minimum in the MoS_2 monolayer, as shown in Fig. 5. Thus, based on the Schottk-Mott rule,[51,52] the *n*-type Schottky barrier height can be calculated as follows: $\Phi_{B,n} = W_G - \chi - (W_G - W_{MoS_2}) = W_{MoS_2} - \chi = E_{vac}^{MoS_2} - E_F - (E_{vac}^{MoS_2} - E_{CBM}) = E_{CBM} - E_F$, where E_{CBM} is the conduction band minimum, $E_{vac}^{MoS_2}$ is the energy of vacuum level of MoS_2 monolayer. Similarly, if $\Delta W < 0$, the *p*-type Schottky barrier height is calculated as:[53] $\Phi_{B,p} = I_{MoS_2} - \chi - W_G = E_F - E_{VBM}$, as shown in Fig. 5(b). Therefore, the *n*-type Schottky barrier height (SBH) of G/MoS_2 interface can be defined as the energy difference between the conduction band minimum (CBM) of the MoS_2 monolayer and the Dirac point of the graphene layer (E_F) and the *p*-type SBH is defined as the energy difference between the Dirac point of the graphene layer and the valence band maximum (VBM) of the MoS_2 monolayer. This Schottky-Mott rule has also been successfully used to calculate the SBH of the metal/semiconductor interfaces, such as graphene/phosphorene,[26] graphene/arsenene,[54] graphene/g-GaN,[55] and graphene/SnS.[42] As shown in Fig. 4, we found the *n*-type Schottky barriers of 0.482 eV, 0.472 eV, 0.474 eV, and

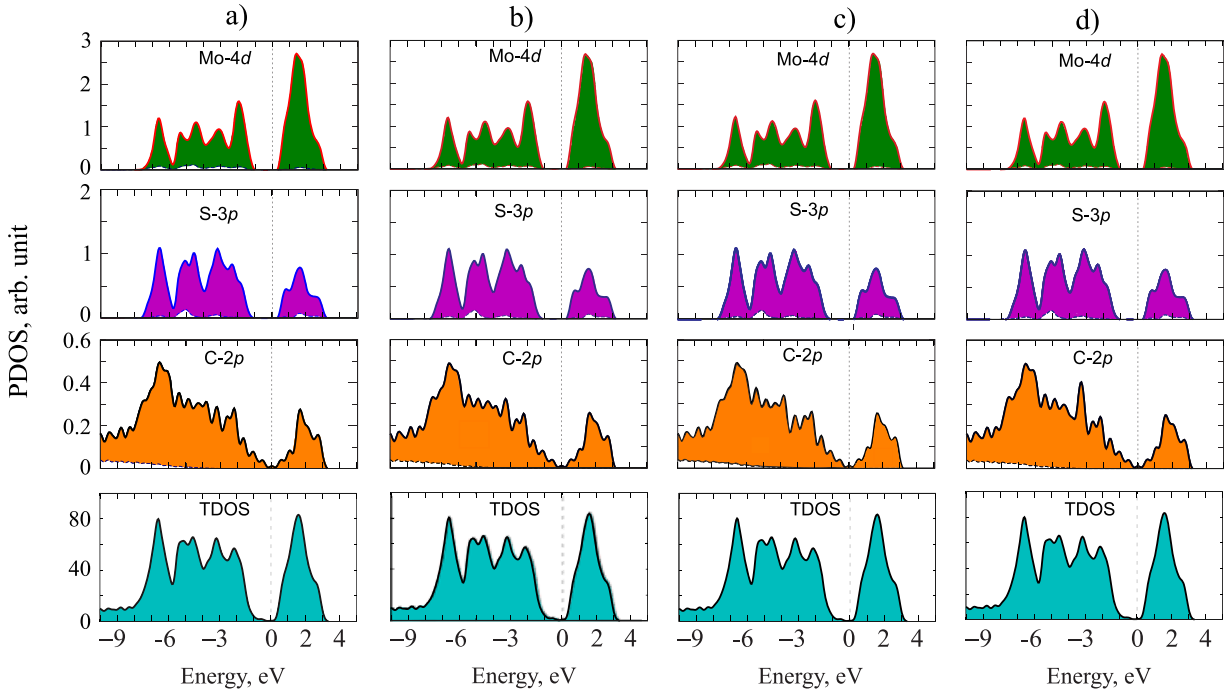

FIG. 6. Projected density of states of Mo, S, and C atoms in G/MoS_2 interface with different stacking configurations: (a) GS-M configuration, (b) GM-S configuration, (c) GS-G configuration, and (d) GM-G configuration.

0.486 eV corresponding to the GM-S, GS-M, GM-G, and GS-G stacking configurations, respectively. These results are in good agreement with the previous data of $\Phi_{B,n} = 0.49$ eV.[56] Also, these small values of the SBH indicate a low on/off threshold voltage which can be prospective for low power consumption electronic devices.

The projected density of states (PDOS) of Mo-4*d*, S-3*p*, and C-2p_z orbital states and the total DOS in the G/MoS_2 interfaces are shown in Fig. 6. Compared to the projected density of state of freestanding graphene, we found that the PDOS of C-2p_z orbitals in the G/MoS_2 interface was almost not changed due to the weak interaction between graphene and MoS_2 monolayer. However, compared to the PDOS of S-3*p* and Mo-4*d* in monolayer MoS_2, it indicates that the valence/conduction bands of S-3*p* and Mo-4*d* near the Fermi level are moved upward to/from the Fermi level in G/MoS_2 interface. The shifted energy for the VBM and the CBM for G/MoS_2 interfaces is about 0.37 eV as shown in Fig. 6. Note that the C-*p*-orbital in graphene and Mo-*d*-orbital in MoS_2 monolayer, which are maximum contributors for the Dirac cone in graphene and VBM, CBM positions in MoS_2, respectively, are used to study these changes.

IV. CONCLUSION

In summary, we have investigated the atomic and electronic properties of G/MoS_2 interfaces within the framework of density functional theory for four different stacking configurations of interfaces. Our calculations indicate that the interaction between graphene and MoS_2 monolayer is the weak van der Waals interaction. The interlayer distance between graphene and MoS_2 monolayer is about 3.34 Å, and the binding energy per C atoms is about −32.4 meV. The electronic properties of G/MoS_2 interfaces seem to be a simple sum of each constituent. The linear Dirac-like dispersion relation around the Fermi level of graphene is still preserved in G/MoS_2 interface. However, focusing on the linear dispersion, we found that the band gap about 3 meV of G/MoS_2 interface is opened at the Dirac *K*-point of graphene. The band gap opening in G/MoS_2 interface can be explained as the lattice symmetry between graphene and MoS_2 monolayer. The appearance of the energy band gap of graphene has opened up new possibilities for using it in graphene-based device applications. In addition, we found that an *n*-type Schottky contact is formed at the G/MoS_2 interface in all four stacking configurations with a small Schottky barrier about 0.49 eV.

ACKNOWLEDGMENTS

This research was funded by Vietnam National Foundation for Science and Technology Development (NAFOSTED) under Grant No. 103.01-2016.07 and the Belarusian scientific program "Convergence."

[1]K. Novoselov, A. K. Geim, S. Morozov, D. Jiang, M. Katsnelson, I. Grigorieva, S. Dubonos, and A. Firsov, Nature **438**, 197 (2005).
[2]A. K. Geim and I. V. Grigorieva, Nature **499**, 419 (2013).
[3]A. K. Geim and K. S. Novoselov, Nat. Mater. **6**, 183 (2007).
[4]K. S. Novoselov, A. K. Geim, S. V. Morozov, D. Jiang, Y. Zhang, S. V. Dubonos, I. V. Grigorieva, and A. A. Firsov, Science **306**, 666 (2004).
[5]A. H. Castro Neto, F. Guinea, N. M. R. Peres, K. S. Novoselov, and A. K. Geim, Rev. Mod. Phys. **81**, 109 (2009).
[6]A. Katanin, Phys. Rev. B **88**, 241401 (2013).
[7]G. Berdiyorov, H. Bahlouli, and F. Peeters, Physica E **84**, 22 (2016).
[8]C. Park, J. Ryou, S. Hong, B. G. Sumpter, G. Kim, and M. Yoon, Phys. Rev. Lett. **115**, 015502 (2015).
[9]L. Liao, J. Bai, Y. Qu, Y. Huang, and X. Duan, Nanotechnology **21**, 015705 (2010).
[10]B. Huang, Q. Xu, and S.-H. Wei, Phys. Rev. B **84**, 155406 (2011).
[11]J. Zhang, W. Xie, X. Xu, S. Zhang, and J. Zhao, Chem. Mater. **28**, 5022 (2016).
[12]J. Wilson and A. Yoffe, Adv. Phys. **18**, 193 (1969).
[13]C. V. Nguyen and N. N. Hieu, Chem. Phys. **468**, 9 (2016).
[14]C. Ataca, H. Sahin, and S. Ciraci, J. Phys. Chem. C **116**, 8983 (2012).
[15]C. V. Nguyen, V. V. Ilyasov, H. V. Nguyen, and H. N. Nguyen, Mol. Simul. **43**, 86 (2017).
[16]K. F. Mak, C. Lee, J. Hone, J. Shan, and T. F. Heinz, Phys. Rev. Lett. **105**, 136805 (2010).
[17]B. Radisavljevic, A. Radenovic, J. Brivio, V. Giacometti, and A. Kis, Nat. Nanotechnol. **6**, 147 (2011).
[18]Y. Yoon, K. Ganapathi, and S. Salahuddin, Nano Lett. **11**, 3768 (2011).
[19]D. Jena and A. Konar, Phys. Rev. Lett. **98**, 136805 (2007).
[20]C. R. Dean, A. F. Young, I. Meric, C. Lee, L. Wang, S. Sorgenfrei, K. Watanabe, T. Taniguchi, P. Kim, K. L. Shepard, and J. Hone, Nat. Nanotechnol. **5**, 722 (2010).
[21]J. Xue, J. Sanchez-Yamagishi, D. Bulmash, P. Jacquod, A. Deshpande, K. Watanabe, T. Taniguchi, P. Jarillo-Herrero, and B. J. LeRoy, Nat. Mater. **10**, 282 (2011).
[22]G. Giovannetti, P. A. Khomyakov, G. Brocks, P. J. Kelly, and J. Van Den Brink, Phys. Rev. B **76**, 073103 (2007).
[23]P. Xu, Q. Tang, and Z. Zhou, Nanotechnology **24**, 305401 (2013).
[24]T. Kavitha, A. I. Gopalan, K.-P. Lee, and S.-Y. Park, Carbon **50**, 2994 (2012).
[25]Y. Cai, G. Zhang, and Y.-W. Zhang, J. Phys. Chem. C **119**, 13929 (2015).
[26]W. Hu, T. Wang, and J. Yang, J. Mater. Chem. C **3**, 4756 (2015).
[27]G.-C. Guo, D. Wang, X.-Lin Wei, Q. Zhang, H. Liu, W.-M. Lau, and L.-M. Liu, J. Phys. Chem. Lett. **6**(24), 5002–5008 (2015).
[28]M. Ghorbani-Asl, P. D. Bristowe, K. Koziol, T. Heine, and A. Kuc, 2D Mater. **3**, 025018 (2016).
[29]Y. Ma, Y. Dai, M. Guo, C. Niu, and B. Huang, Nanoscale **3**, 3883 (2011).
[30]V. V. Ilyasov, B. Meshi, I. Popova, I. V. Ershov, N. N. Hieu, and C. V. Nguyen, Comput. Theor. Chem. **1098**, 22 (2016).
[31]A. D. Phan, N. A. Viet, N. A. Poklonski, L. M. Woods, and C. H. Le, Phys. Rev. B **86**, 155419 (2012).
[32]W. J. Yu, Z. Li, H. Zhou, Y. Chen, Y. Wang, Y. Huang, and X. Duan, Nat. Mater. **12**, 246 (2013).
[33]M. S. Choi, G.-H. Lee, Y.-J. Yu, D.-Y. Lee, S. H. Lee, P. Kim, J. Hone, and W. J. Yoo, Nat. Commun. **4**, 1624 (2013).
[34]K. Roy, M. Padmanabhan, S. Goswami, T. P. Sai, G. Ramalingam, S. Raghavan, and A. Ghosh, Nat. Nanotechnol. **8**, 826 (2013).
[35]V. V. Ilyasov, B. C. Meshi, V. C. Nguyen, I. V. Ershov, and D. C. Nguyen, J. Appl. Phys. **115**, 053708 (2014).
[36]V. V. Ilyasov, C. V. Nguyen, I. V. Ershov, and N. N. Hieu, J. Appl. Phys. **117**, 174309 (2015).
[37]V. V. Ilyasov, C. V. Nguyen, I. V. Ershov, and N. N. Hieu, RSC Adv. **5**, 49308 (2015).
[38]V. Ilyasov, C. V. Nguyen, I. Ershov, C. D. Nguyen, and N. N. Hieu, Mater. Chem. Phys. **154**, 78 (2015).
[39]P. Giannozzi, S. Baroni, N. Bonini, M. Calandra, R. Car, C. Cavazzoni, D. Ceresoli, G. L. Chiarotti, M. Cococcioni, I. Dabo, A. D. Corso, S. de Gironcoli, S. Fabris, G. Fratesi, R. Gebauer, U. Gerstmann, C. Gougoussis, A. Kokalj, M. Lazzeri, L. Martin-Samos, N. Marzari, F. Mauri, R. Mazzarello, S. Paolini, A. Pasquarello, L. Paulatto, C. Sbraccia, S. Scandolo, G. Sclauzero, A. P. Seitsonen, A. Smogunov, P. Umari, and R. M. Wentzcovitch, J. Phys.: Condens. Matter **21**, 395502 (2009).
[40]J. P. Perdew, K. Burke, and M. Ernzerhof, Phys. Rev. Lett. **77**, 3865 (1996).
[41]S. Grimme, J. Comput. Chem. **27**, 1787 (2006).
[42]W. Xiong, C. Xia, X. Zhao, T. Wang, and Y. Jia, Carbon **109**, 737 (2016).
[43]E. Wang, X. Lu, S. Ding, W. Yao, M. Yan, G. Wan, K. Deng, S. Wang, G. Chen, L. Ma *et al.*, Nat. Phys. **12**, 1111 (2016).
[44]Z. G. Yu, Y.-W. Zhang, and B. I. Yakobson, J. Phys. Chem. C **120**, 22702 (2016).
[45]Z. Xu and M. J. Buehler, J. Phys.: Condens. Matter **22**, 485301 (2010).
[46]X. Fan, W. Zheng, V. Chihaia, Z. Shen, and J.-L. Kuo, J. Phys.: Condens. Matter **24**, 305004 (2012).

[47]V. Ilyasov, I. Ershov, A. Ilyasov, I. Popova, and C. V. Nguyen, Surf. Sci. **632**, 111 (2015).
[48]T. C. Nguyen, M. Otani, and S. Okada, Phys. Rev. Lett. **106**, 106801 (2011).
[49]E. Kan, H. Ren, F. Wu, Z. Li, R. Lu, C. Xiao, K. Deng, and J. Yang, J. Phys. Chem. C **116**, 3142 (2012).
[50]M. Farmanbar and G. Brocks, Phys. Rev. B **91**, 161304 (2015).
[51]J. Bardeen, Phys. Rev. **71**, 717 (1947).
[52]W. Monch, Rep. Prog. Phys. **53**, 221 (1990).
[53]L.-Y. Gan, Q. Zhang, Y. Cheng, and U. Schwingenschlögl, Phys. Rev. B **88**, 235310 (2013).
[54]W. Li, T.-X. Wang, X.-Q. Dai, X.-L. Wang, Y.-Q. Ma, S.-S. Chang, and Y.-N. Tang, Physica E **88**, 6 (2017).
[55]M. Sun, J.-P. Chou, Q. Ren, Y. Zhao, J. Yu, and W. Tang, Appl. Phys. Lett. **110**, 173105 (2017).
[56]B. Liu, L.-J. Wu, Y.-Q. Zhao, L.-Z. Wang, and M.-Q. Cai, RSC Adv. **6**, 60271 (2016).